

Pitting Corrosion as a Failure Mechanism in Aircraft Panels: A Modelling and Simulation Approach

Krishna Lok Singh 

Structural Integrity Division, CSIR—National Aerospace Laboratories, Bengaluru, India

Email: fatiguefracturemech@gmail.com

How to cite this paper: Singh, K.L. (2025) Pitting Corrosion as a Failure Mechanism in Aircraft Panels: A Modelling and Simulation Approach. *Advances in Aerospace Science and Technology*, 10, 64-79.
<https://doi.org/10.4236/aast.2025.102005>

Received: April 29, 2025

Accepted: June 27, 2025

Published: June 30, 2025

Copyright © 2025 by author(s) and Scientific Research Publishing Inc. This work is licensed under the Creative Commons Attribution International License (CC BY 4.0).
<http://creativecommons.org/licenses/by/4.0/>



Open Access

Abstract

Pitting corrosion is a significant failure mechanism in aging aircraft structures, potentially leading to catastrophic structural failures. This study investigates the stress distribution around idealized cylindrical corrosion pits in aluminium aircraft panels under uniaxial tensile loading using three-dimensional finite element analysis (3D FEA). A systematic approach was employed to analyse the influence of varying pit diameters and depths on stress concentration. The maximum stress concentration was consistently observed at the pit's anterior surface, perpendicular to the loading direction. A novel modified formula was developed to calculate the stress concentration factor (SCF) in pitted panels, considering the remaining material thickness, and providing a more accurate prediction compared to traditional methods. The results revealed a clear relationship between the pit aspect ratio (depth/diameter) and the SCF. A bi-linear material model was implemented to determine the yield strength of the panel under these conditions. The analysis also explored the stress concentrations associated with triangular pit geometries, demonstrating elevated stress levels compared to cylindrical pits of equivalent area. These findings offer critical insights into the structural integrity of aircraft panels affected by pitting corrosion. The proposed novel formula improves the prediction of structural failure and can be applied to enhance design and maintenance protocols in the aerospace industry to improve aircraft longevity and safety.

Keywords

Pitting Corrosion, Failure Analysis, Aircraft Panels, Finite Element Analysis, Stress Concentration Factor

1. Introduction

The structural integrity of aircraft is critical for ensuring safety and operational longevity. Pitting corrosion, a localized form of material degradation, significantly reduces structural strength, leading to increased failure susceptibility. This is particularly relevant in aging aircraft, where fatigue cracks often originate from corrosion pits under cyclic loading [1]. Notable aviation accidents, such as Aloha Airlines Flight 243, have underscored the dangers of corrosion-induced fatigue damage, prompting advancements in inspection and maintenance protocols [2].

Extensive research has demonstrated the detrimental impact of pitting corrosion on the fatigue strength of aerospace materials. Previous studies have demonstrated that pitting corrosion reduces the fatigue strength of aerospace materials, with reported losses of up to 40% under certain fatigue cycles [1] [3]. The primary factors influencing the ultimate strength of corroded panels include pit geometry, depth, and diameter. Furthermore, investigations into the relationship between pit shape and fatigue life have underscored the importance of considering pit morphology when assessing structural durability. Advanced numerical simulations, such as nonlinear finite element analysis, have emerged as reliable tools for assessing structural behaviour, providing credible insights that complement experimental investigations. These simulations inform design modifications aimed at enhancing structural performance and reliability, thereby mitigating the risks associated with corrosion-induced failures. Similarly, the influence of corrosion pits on the residual strength of aircraft panels has been examined, demonstrating a significant reduction in load-carrying capacity due to pitting. Numerical analyses have also explored the effectiveness of cathode protection in preventing corrosion, highlighting novel methodologies for mitigating its effects. In a harsh marine environment, increased stress accelerates corrosion, leading to the formation of corrosion pits and intensifying corrosion at defect sites. While numerical simulations have been used extensively to study stress corrosion cracking (SCC) and corrosion-induced mechanical property degradation (CIMPD), there remains a need for more refined computational models to predict failure mechanisms more accurately. The CIMPD of 7050-T7451 aluminium alloy has also been studied to reveal the controlling steps in the stress-assisted degradation of aluminium alloy [3] [4].

This research addresses the SCC gap by systematically investigating SCF in corroded aircraft panels using finite element analysis (FEA). This research also investigates the impact of stress concentration on isolated cylindrical pits with varying depths and diameters under uniaxial loading through a systematic series of 3-D finite element simulations. The study determines the values of stress concentration factors and aspect ratios (depth/diameter) for different pit configurations. Additionally, nonlinear finite element analysis and fatigue analysis were conducted to evaluate the model's yield strength and service life. By leveraging advanced computational techniques, this research provides a refined framework for predicting failure points in corroded structures, offering both theoretical insights and practical applications for improving aircraft safety and reliability.

2. Methodology

2.1. Finite Element Strategy

The modelling of aircraft structure panel was carried out using ANSYS Workbench environment. Although the geometry of the panel is symmetrical, a full model was used as the quarter model does not render good results. The details of modelling strategies, sizing, and their properties are listed in the following sections.

A 100 mm × 100 mm aluminium panel with a thickness of 2.5 mm was modelled using ANSYS Workbench. Finite element analysis was carried out using ANSYS package. In order to prepare the models, ANSYS “Space Claim geometry” was used. **Figure 1** shows the panel without the corrosion pit formation. **Figure 2** shows the panel with corrosion pit formed.

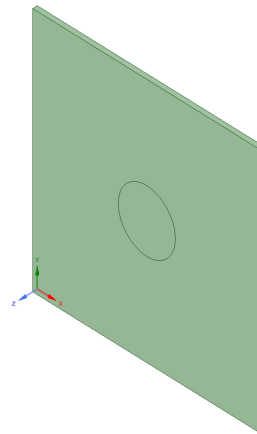


Figure 1. Before formation of corrosion pit.

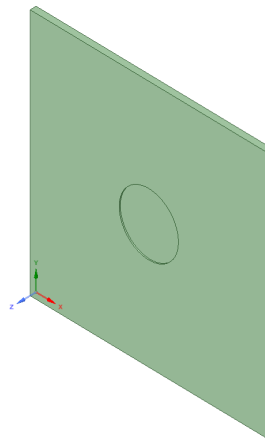


Figure 2. After formation of corrosion pit.

As shown in **Figure 1**, before Boolean operation, a single line indicates the region of the corrosion pit. In **Figure 2**, after the Boolean operation of pull, a circular object of the required diameter of the desired corrosion pit is pulled from the original panel. The double line indicates the presence of the corrosion pit of the de-

sired diameter and at depth.

The finite element mesh was generated using a hex-dominant method, incorporating SOLID186 and SOLID187 elements to enhance computational precision. Both SOLID186 (a quadratic three-dimensional 20-node solid element of higher order) and SOLID187 (a quadratic three-dimensional 10-node solid element of higher order) elements were adopted while meshing the model. The input value for element size was given as 1mm to obtain a fine mesh for accurate results. A mesh convergence study was performed to ensure the result was independent of mesh size.

2.2. Material Properties

Both linear and nonlinear material models were considered. The elastic modulus was set at 71 GPa, with a Poisson's ratio of 0.33. Nonlinear analysis was conducted using a bilinear model with a tangent modulus of 500 MPa to capture material yielding behaviour under applied loads. In order to run the simulation ANSYS "Static Structural" analysis system is used.

2.3. Boundary Conditions and Loading

Tensile loads ranging from 10 KN to 80 KN were applied to one edge, while the opposite edge was constrained in the x-direction ($U_x = 0$). This setup ensured realistic simulation conditions aligned with typical aircraft panel loading scenarios.

Figure 3 shows the panel with both the loading and displacement boundary conditions. On one edge, tensile loads of magnitude ranging from 10 KN to 80 KN in increments of 10 KN were applied and on the opposite edge the displacement constraint of $U_x = 0.0$ was applied.

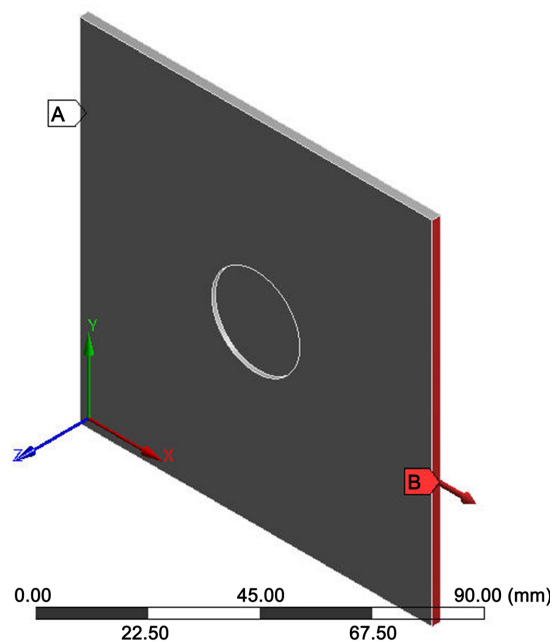


Figure 3. Model with boundary conditions applied.

Initially from the simulation point of view, a tensile load of 10 KN was applied on the boundary with the intent of preserving the values of stress below the yield strength of material. The finite element analysis was performed and the values of stress concentration factors were calculated for panels having different pit geometries. The pit diameters considered in this paper have values ranging from 6 mm to 75 mm. And the values of pit depths varied from 0.5 mm to 2 mm.

3. Results and Discussions

All the simulations performed used ANSYS software package, for both the static and nonlinear analyses. The results and discussion are given in the following sections.

3.1. Stress Concentration Factor (SCF) in Corroded Panels

The data in **Tables 1-4** show the values of maximum equivalent von-Mises stresses obtained for different geometries of the pit. Precisely the values of pit diameters considered for the analysis were 6, 15, 25, 50 and 75 mm and those of pit depths were 0.5, 1, 1.5 and 2 mm respectively. Normally, to calculate the stress concentration factor (SCF) values for a plate without a hole or pit, the following formulas are used:

$$\sigma_{\text{nom}} = \frac{F}{W \times t} \quad (1)$$

This is the applied stress, applicable for no damage panel. **Figure 4** and **Figure 5** represent the effect of diameter and depth location of the pit; here, it is observed that the values of SCF are high.

Once there is a hole type of discontinuity then the formula for the computation of nominal stress is:

$$\sigma_{\text{nom}} = \frac{F}{(W - D) \times t} \quad (2)$$

where, F is the load applied in KN, W = plate width (mm), D = pit diameter (mm), t = plate thickness (mm).

Figure 6 shows the values of stress concentration factors for different pit diameters.

The formula to compute stress concentration factor does not change either for a damaged or an undamaged panel. The formula for the Stress Concentration Factor is:

$$K_t = \frac{\sigma_{\text{max}}}{\sigma_{\text{nom}}} \quad (3)$$

where K_t is the stress concentration factor.

But in the case of pits, the formula used above cannot be used as it does not consider the thickness of the panel excluding the pit depth. As a result, an attempt has been made to develop an expression that can be used to calculate the stress concentration factor for pitted panels. The modified novel formula for pitted pan-

els is stated in next section.

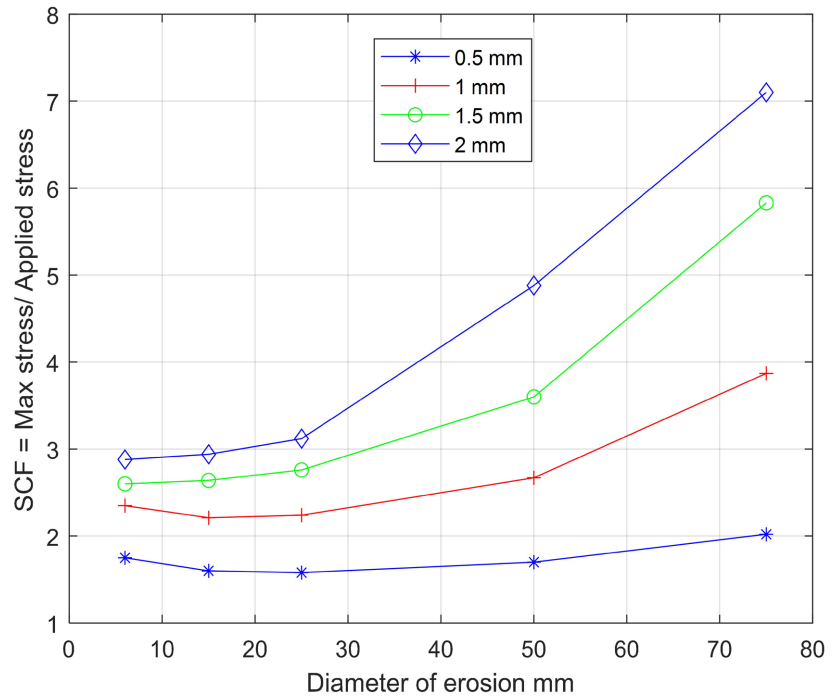


Figure 4. SCF versus diameter of erosion for different pit depths.

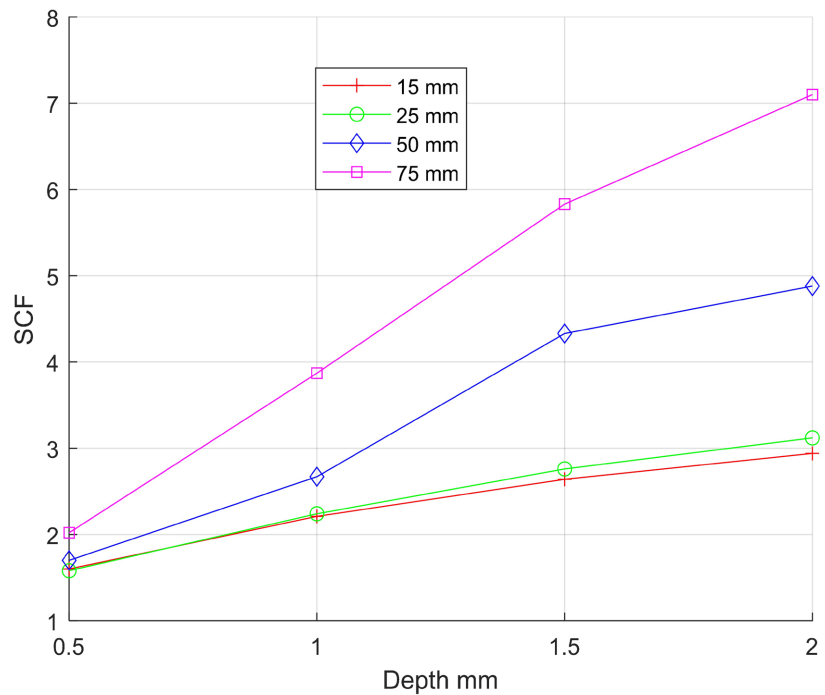


Figure 5. SCF versus depth of erosion for different pit diameters.

The erosion is formed due to pit corrosion and the remaining portion of the panel is considered in this novel modified formula. The additional term comes in

the denominator of the nominal stress computation, as shown in Equation (4). The SCF computation is the same as in Equation (3). The novel modified formula for nominal stress is as follows,

$$\sigma_{\text{nom}} = \frac{F}{(W - D) \times t + (D \times r_t)} \quad (4)$$

W = plate width (mm);

D = pit diameter (mm);

T = plate thickness (mm);

r_t = remaining thickness of the panel at the location of pit.

Figure 6 depicts the values of the stress concentration factor versus various diameters at different depths using the novel modified formula. It is observed that the SCF values decrease when we use Equation (4).

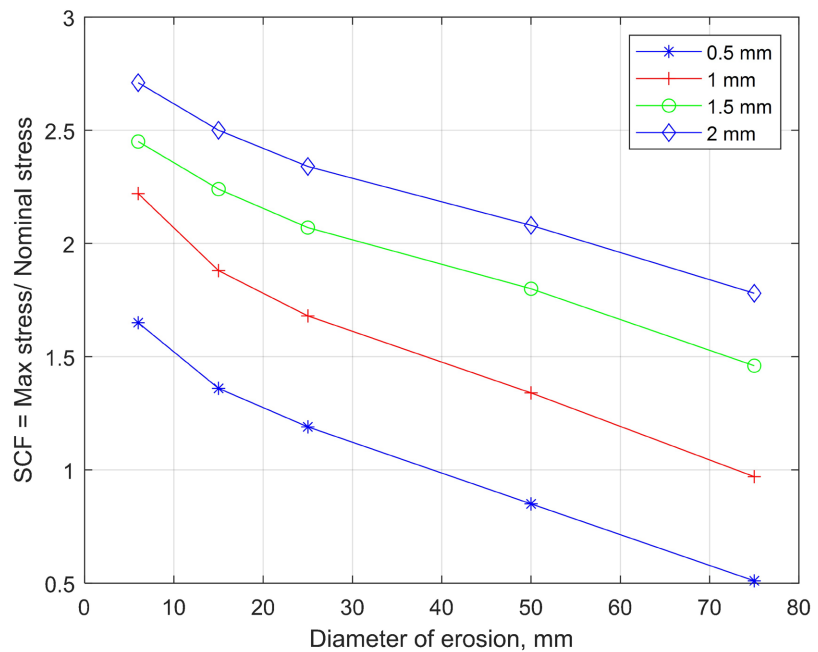


Figure 6. Computation of SCF using nominal stress formula.

The data in **Tables 1-4** show the values of maximum equivalent von-Mises stresses obtained for different geometries of the pit. Precisely the values of pit diameters (D) considered for the analysis were 6, 15, 25, 50 and 75 mm and those of pit depths (d) were 0.5, 1, 1.5 and 2 mm respectively. The load applied was 10 kN with boundary conditions as defined above. This particular boundary condition displayed the highest stress concentration in the upper margin of pit which is shown in **Figure 7**.

$$\text{Aspect Ratio (AR)} = \frac{d}{D} \quad (5)$$

d = pit depth (mm);

D = pit diameter (mm).

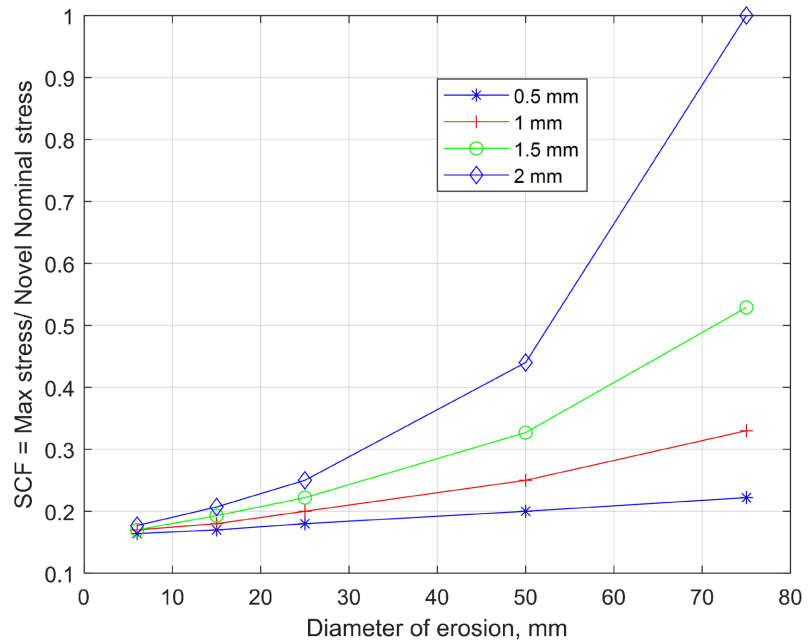


Figure 7. Computation of SCF using Novel modified nominal stress formula.

Table 1. Values of stress, SCF and AR for panels with $d = 0.5$ mm.

Diameter (D, mm)	von-Mises stress (MPa)	SCF	AR
6	70.155	1.73	0.083
15	64.178	1.56	0.033
25	63.302	1.51	0.020
50	68.298	1.54	0.010
75	81.050	1.73	0.006

Table 2. Values of stress, SCF and AR for panels with $d = 1$ mm.

Diameter (D, mm)	von-Mises stress (MPa)	SCF	AR
6	94.233	2.30	0.166
15	88.599	2.08	0.066
25	89.799	2.02	0.040
50	107.09	2.14	0.020
75	155.12	2.72	0.013

Table 3. Values of stress, SCF and AR for panels with $d = 1.5$ mm.

Diameter (D, mm)	von-Mises stress (MPa)	SCF	AR
6	104.380	2.52	0.250
15	105.550	2.40	0.100
25	110.310	2.35	0.060
50	144.010	2.52	0.030
75	233.280	3.22	0.020

Table 4. Values of stress, SCF and AR for panels with $d = 2$ mm.

Diameter (D, mm)	von-Mises stress (MPa)	SCF	AR
6	115.120	2.74	0.333
15	117.460	2.58	0.133
25	124.810	2.50	0.080
50	166.400	2.49	0.040
75	284.250	2.84	0.026

From the values obtained in the tables above it can be observed that the values of SCF decrease with increase in diameter for the same depth. **Figure 4** and **Figure 5** show the plots of SCF versus pit diameters and depths respectively. **Figure 7** shows the plots of depth versus SCF for pit diameters of 0.05 mm to 1 mm using novel modified formula (4).

The plots in **Figure 4** and **Figure 5** show that as the diameter of the pit grows, so does the value of SCF. In **Figure 6** it is observed that the SCF decreases with the nominal formula computation. However, in **Figure 7** the trend of increasing SCF is seen with the novel modified formula. It is recommended that the novel modified formula be used for the computation of SCF for this type of pitting corrosion problem.

Once the relationship between SCF, pit diameter and pit depth were established, efforts were made to determine the relation between SCF and AR and also to determine the yield strength of the plate. Non-linear analysis was performed using bi-linear material theory to determine the yield strength of the plate. **Figure 8** shows the nature of a bi-linear graph. The intersection of the two curves indicates the yield point of the model.

Based on this theory, bi-linear analysis was conducted for the model under evaluation to derive the stress-strain curve and calculate the yield strength. Tensile load was applied on one edge of the model with displacement boundary condition ($x = 0$) on the other edge. The magnitude of loads varied from 10 KN to 80 KN with an increment of 10 KN for each system. **Table 5** displays the maximum von-Mises stress and directional deformation values for various loads.

Table 5. Values of maximum von-Mises stress and directional deformation from bi-linear analysis.

Load (KN)	von-Mises stress (MPa)	Deformation (mm)
10	40.015	0.05637
20	80.059	0.11282
30	120.130	0.16935
40	160.240	0.22594
50	200.370	0.28261
60	240.540	0.33936
70	281.670	0.73056
80	454.38	42.3360

The stress-strain curves of alloy AA6082 tempers T4 and T6 were found by standard tensile testing, and fitted to the five-parameter model

$$\sigma = \sigma_0 + Q_1 \left(1 - \exp(-C_1 \varepsilon^p)\right) + Q_2 \left(1 - \exp(-C_2 \varepsilon^p)\right) \quad (6)$$

where σ is the stress; $\varepsilon^p = \varepsilon - \sigma/E$ is the plastic strain; ε is the total strain; E is Young's modulus; σ_0 , Q_k and C_k ($k = 1, 2$) are material constants. The stress-strain curve up to 1% plastic strain was used to calibrate Equation (1). The computed $f_{0.2}$ is the yield stress (defined as the stress at 0.2% plastic strain), which matches with our FEA values [5].

The pit size was found to increase with time (t) following the relation [6]: Pit size $\propto t^{1/3}$.

The impact of pitting corrosion upon the fatigue behaviour of exposed 7075-T6 aluminium alloy reduced its fatigue life by a factor of 6 to 8 [7] [8]. The fatigue life of plates with corrosion is studied using a neural network model developed by Pidaparti *et al.* [9]. The findings were cross-checked against analysis and laboratory data. The fatigue life estimate derived from the current approach can be used to help evaluate the remaining life or to schedule the next examination in the maintenance program.

Recent research [10] has also investigated the use of advanced finite element techniques to simulate the stress distribution around corrosion pits, offering insights into the mechanisms of crack initiation and propagation. Finally, recent numerical analysis by Sankaran *et al.* [11] investigated the effectiveness of using cathodic protection on preventing corrosion, highlighting a novel methodology. In a research work [12], a specific aluminum alloy (7075-T6) holds up to fatigue (repeated stress) when it has multiple holes, like those used in aircraft construction. It also examines how corrosion affects this material. The study found that while a technique called "cold expansion" can improve the material's resistance to fatigue, corrosion can still significantly reduce its lifespan, especially in the early stages of exposure.

3.2. Influence of Pit Geometry on Stress Distribution

The research [13] [14] examines how stress influences the corrosion of a specific aluminum alloy (7050) in a simulated harsh marine environment. It demonstrates that increased stress accelerates corrosion, leading to the formation of corrosion pits. The study also explores how stress concentration at corrosion defects further intensifies corrosion and how different levels of stress affect the corrosion mechanism.

It is important to investigate the impact of stress concentration for triangular geometry of pit because development of pitting corrosion leads to crack formation [14]. The area of the triangle is equal to the area of a circle (491 mm²) with a 25 mm diameter and the pit depth considered is 1.5 mm. The crack originates from the conical shape only. As we see in **Figure 8**, the cylindrical pit has maximum stress of 110 MPa, whereas the conical or triangle geometry has 157 MPa (**Figure 9**). The stress values of triangular pits are more by 30% in comparison with cylindri-

cal pits of the same area. Athanasios Kolios *et al.* [13] made similar observations but for conical pits.

Comparative analysis of cylindrical and triangular pit geometries revealed that triangular pits exhibited stress values approximately 30% higher than cylindrical pits of equivalent cross-sectional area. This finding highlights the necessity of considering pit shape variations in failure analysis.

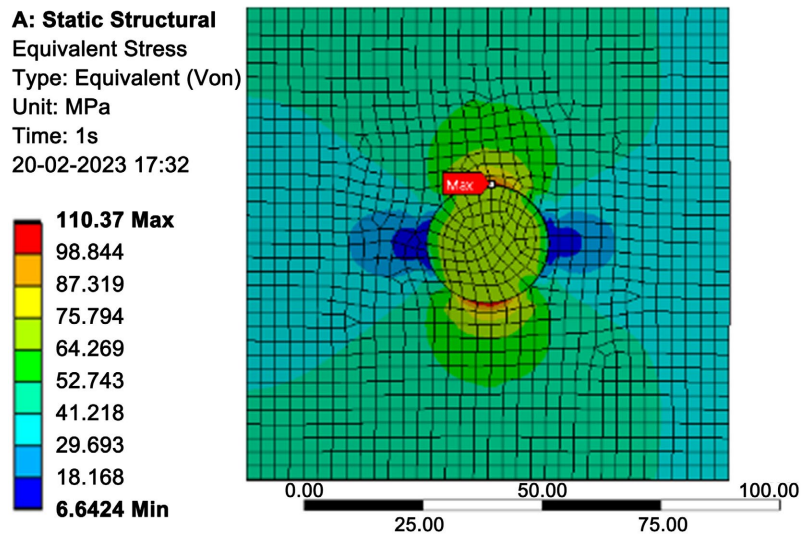


Figure 8. Stress pattern of circular pit.

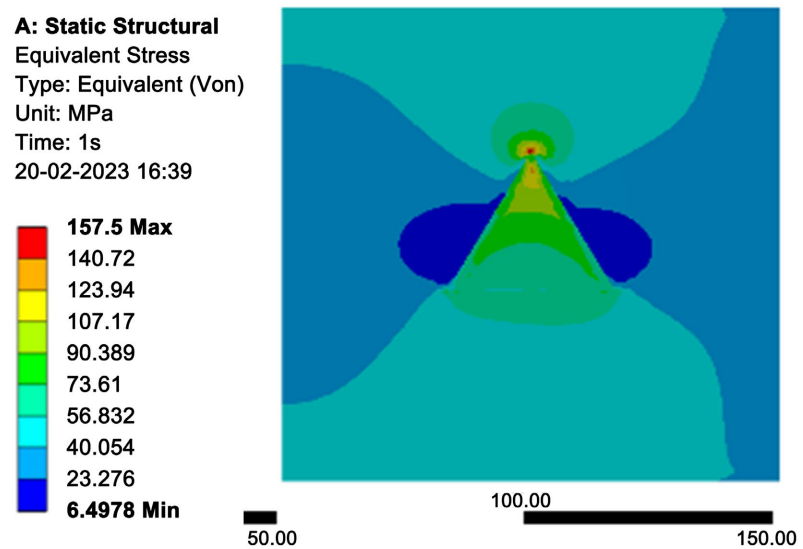


Figure 9. Stress pattern of triangle pit.

3.3. Yield Strength and Structural Integrity

A bi-linear stress-strain curve was generated from nonlinear FEA, determining the panel's yield strength at approximately 248 MPa. Load-deformation analysis indicated that panels with pit depths greater than 2 mm or diameters exceeding 75 mm experienced significant reductions in load-bearing capacity, confirming

that such corrosion levels are structurally unacceptable under operational conditions.

Figure 10 and **Figure 11** show the bi-linear graphs obtained for the panel for two load cases, 70 KN and 80 KN respectively. From **Table 5**, one can observe that up to the load of 70 KN, the values of stress and deformation increased linearly with an increase in load. When the load applied was 80 KN the values of stress and deformation increased drastically depicting that the strength of panel has passed the yield point. On comparing **Figure 8** and **Figure 9**, we can conclude that the yield strength of the model corresponds to the point marked in red having a value of around 248 MPa.

After obtaining the value of yield strength of the panel two graphs were plotted as shown in **Figure 12** and **Figure 13** to indicate the maximum allowable pit depth and diameter, *i.e.*, the permissible values of dimensions of pit diameter and depth above which failure of the plate occurs.

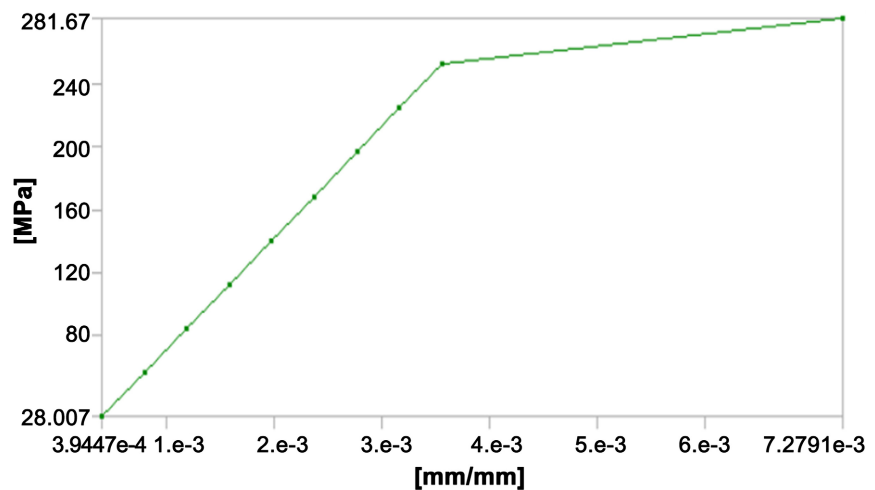


Figure 10. Bi-linear curve for 70 KN load case.

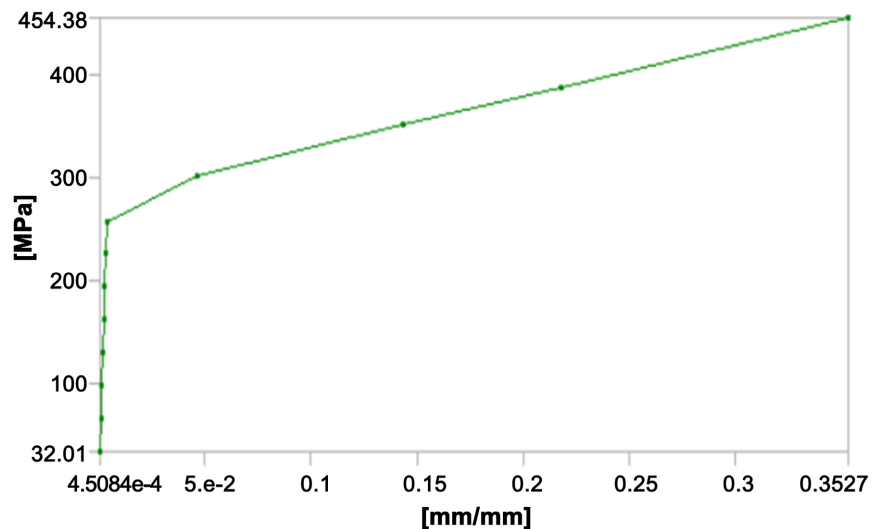


Figure 11. Bi-linear curve for 80 KN load case.

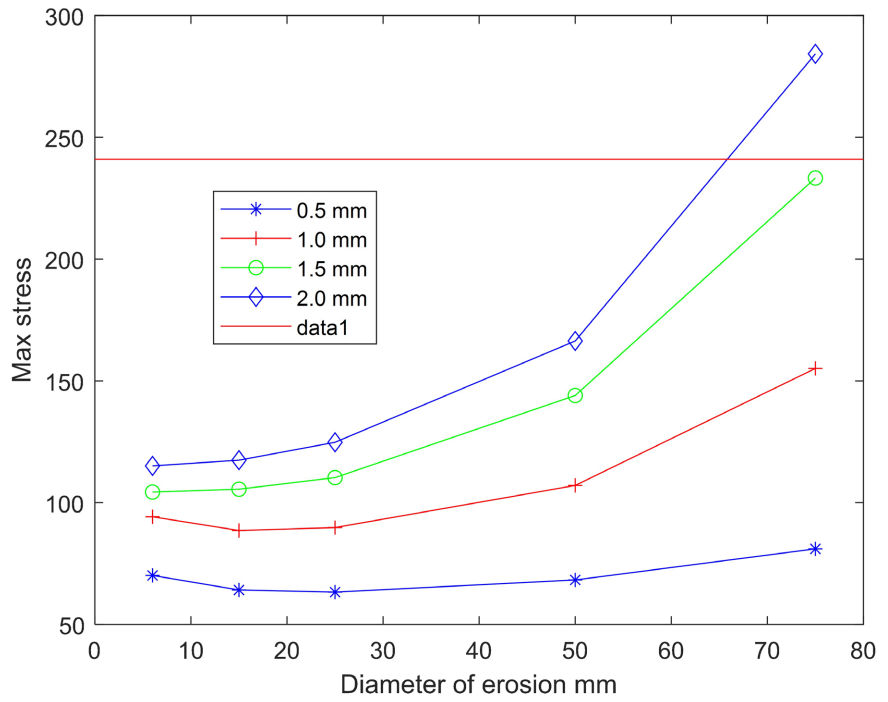


Figure 12. Indication of maximum depth allowable.

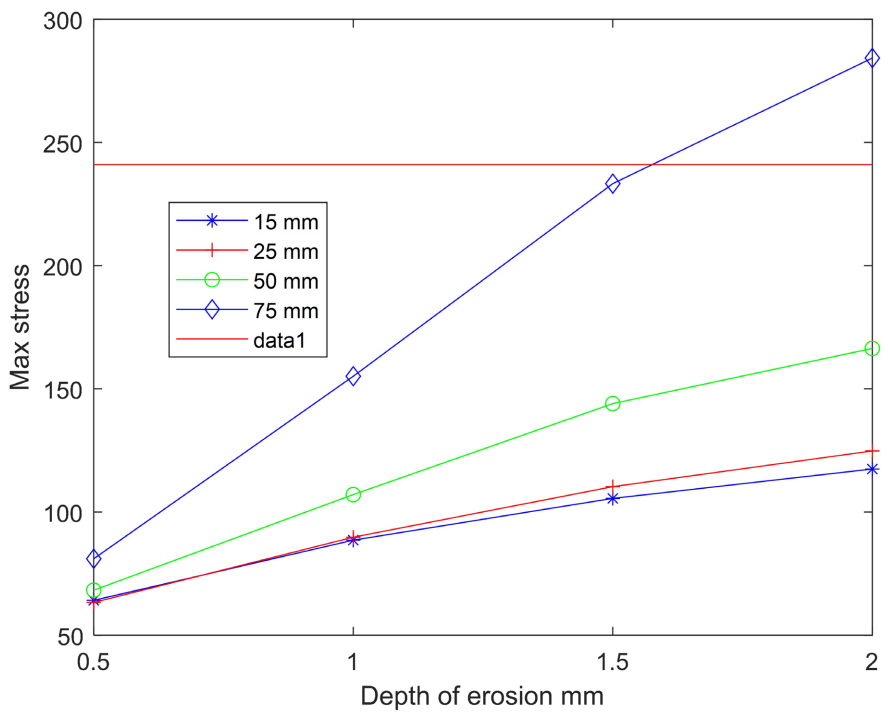


Figure 13. Indication of maximum diameter allowable.

From these plotted figures, it can be concluded that pit depths greater than 1.6 mm or diameters exceeding 65 mm experienced significant reductions in load-bearing capacity, confirming that such corrosion levels are structurally unacceptable under operating conditions.

4. Reviewer's Comments Answers

Experimental and numerical studies have shown that the SCF for corrosion pits in aluminium alloys typically ranges from 1.5 to 3, depending on pit aspect ratio (depth/diameter), pit size, and loading conditions. For example, pre-pitted samples with a pit aspect ratio of 0.11 demonstrated an SCF of around 1.5, which led to a reduction in fatigue life by over 60% compared to un-pitted samples [15]. **Table 6** depicts representative literature to answer reviewer comments.

The novel SCF formula presented in the attached paper aligns with established literature benchmarks in terms of the relationship between pit geometry, SCF, and fatigue life reduction. The SCF values and trends predicted by the new formula fall within the ranges reported by experimental and numerical studies in the literature. However, as noted previously, the direct validation of the novel formula against new physical test data is not explicitly reported; rather, its credibility is supported by consistency with these well-established benchmarks [15]-[17].

Table 6. Representative literature examples.

Reference	Key Finding
[15]	Pitting corrosion reduced fatigue life by a factor of 6 - 8 in aluminum alloys.
[16]	Pre-pitted samples (aspect ratio 0.11, SCF \approx 1.5) had fatigue lives reduced by >60%.
[17]	Pit depth is the dominant factor for fatigue life; empirical models validated with teardown data.
[18]	Stress concentration from pits leads to reduced elongation and earlier failure.
[19]	Classification and fatigue life of pitting corrosion in aircraft materials; S-N data for pitted vs. unpitted samples.

5. Conclusions and Recommendations

This study provides a refined framework for evaluating pitting corrosion-induced failures in aircraft panels. Key findings include:

- 1) The novel modified SCF formula enhances failure prediction accuracy.
- 2) Triangular pits exhibit significantly higher stress concentrations than cylindrical pits.
- 3) Corrosion pits with diameters exceeding 65 mm or depths beyond 1.6 mm lead to substantial structural degradation. Hence, beyond these sizes are not recommended for usage.
- 4) Crack grows from the sharp edges; hence, the need to simulate conical-type geometries is essential. Modelling and simulation of triangle geometry is simulated, and it shows that 30% higher stress occurs in the case of conical type geometry than in circular geometry.
- 5) The values of stress and strain increase linearly with an increase in depth. The values of stress increase with increases in depth of erosion and the values of diameter increase in an exponential way.

Future work should focus on integrating fatigue and buckling analyses to further assess the long-term performance of corroded panels. Additionally, experimental validation of the proposed SCF formula through mechanical testing would strengthen its applicability in real-world aerospace engineering scenarios.

Acknowledgements

The author extends gratitude to the Director, and Head of the Structural Integrity Division at the Council of Scientific and Industrial Research – National Aerospace Laboratories (CSIR-NAL) for their continuous support. Special thanks are also due to colleagues who contributed directly or indirectly to the computational and analytical aspects of this study.

Conflicts of Interest

The author declares no conflicts of interest regarding the publication of this paper.

References

- [1] Arunachalam, A.P.S. (2009) Effect of Pitting Corrosion on Ultimate Strength and Buckling Strength of Plates—A Review. *Digest Journal of Nanomaterials and Biostructures*, **4**, 783-788.
- [2] Pitt, S. and Jones, R. (1997) Multiple-Site and Widespread Fatigue Damage in Aging Aircraft. *Engineering Failure Analysis*, **4**, 237-257. [https://doi.org/10.1016/s1350-6307\(97\)00020-4](https://doi.org/10.1016/s1350-6307(97)00020-4)
- [3] Colvin, E.L., Kulak, M., Bray, G.H. and Bucci, R.J. (1997) Effects of Prior Corrosion on the S-N Fatigue Performance of Aluminum Alloys 2024-T3 and 2524-T3. Effects of Environment on the Initiation of Crack Growth ASTM STP 1298, ASTM.
- [4] Wu, H., Wang, M., Bian, G., Xin, Y., Wang, L., Meng, D., *et al.* (2025) Comparative Study of Stress Corrosion Cracking and Corrosion-Induced Mechanical Property Degradation of 7050-T7451 Aluminum Alloy in Chloride Solution Containing Bisulfite. *Engineering Failure Analysis*, **167**, Article109054. <https://doi.org/10.1016/j.engfailanal.2024.109054>
- [5] Hopperstad, O.S., Langseth, M. and Hanssen, L. (1997) Ultimate Compressive Strength of Plate Elements in Aluminium: Correlation of Finite Element Analyses and Tests. *Thin-Walled Structures*, **29**, 31-46. [https://doi.org/10.1016/s0263-8231\(97\)00013-x](https://doi.org/10.1016/s0263-8231(97)00013-x)
- [6] Kondo, Y. (1989) Prediction of Fatigue Crack Initiation Life Based on Pit Growth. *Corrosion*, **45**, 7-11. <https://doi.org/10.5006/1.3577891>
- [7] Genel, K., Demirkol, M. and Gülmez, T. (2000) Corrosion Fatigue Behaviour of Ion Nitrided AISI 4140 Steel. *Materials Science and Engineering: A*, **288**, 91-100. [https://doi.org/10.1016/s0921-5093\(00\)00835-2](https://doi.org/10.1016/s0921-5093(00)00835-2)
- [8] Miller, B.A., Shipley, R.J., Parrington, R.J. and Dennies, D.P. (1995) Metals Handbook. Failure Analysis and Prevention. Fatigue Failure. Vol. 11. ASM Int Metals Park.
- [9] Pidaparti, R.M., Jayanti, S., Sowers, C.A. and Palakal, M.J. (2002) Classification, Distribution, and Fatigue Life of Pitting Corrosion for Aircraft Materials. *Journal of Aircraft*, **39**, 486-492. <https://doi.org/10.2514/2.2954>
- [10] Fu, J., Zhang, T., Wang, C., Chen, C., Zhang, T. and He, Y. (2024) Effect of Cold Expansion on the Fatigue Life of Multi-Hole 7075-T6 Aluminum Alloy Structures under

- the Pre-Corrosion Condition. *Engineering Failure Analysis*, **165**, Article 108812. <https://doi.org/10.1016/j.engfailanal.2024.108812>
- [11] Sankaran, K.K., Perez, R. and Jata, K.V. (2001) Effects of Pitting Corrosion on the Fatigue Behavior of Aluminum Alloy 7075-T6: Modeling and Experimental Studies. *Materials Science and Engineering: A*, **297**, 223-229. [https://doi.org/10.1016/s0921-5093\(00\)01216-8](https://doi.org/10.1016/s0921-5093(00)01216-8)
- [12] Cerit, M., Genel, K. and Eksi, S. (2009) Numerical Investigation on Stress Concentration of Corrosion Pit. *Engineering Failure Analysis*, **16**, 2467-2472. <https://doi.org/10.1016/j.engfailanal.2009.04.004>
- [13] Kolios, A., Srikanth, S. and Saloniitis, K. (2014) Numerical Simulation of Material Strength Deterioration Due to Pitting Corrosion. *Procedia CIRP*, **13**, 230-236. <https://doi.org/10.1016/j.procir.2014.04.040>
- [14] Yan, X., Rong, H., Fan, W., Yang, J., Zhou, C., Li, S., *et al.* (2024) Effect and Simulation of Tensile Stress on Corrosion Behavior of 7050 Aluminum Alloy in a Simulated Harsh Marine Environment. *Engineering Failure Analysis*, **156**, Article 107843. <https://doi.org/10.1016/j.engfailanal.2023.107843>
- [15] Rokhlin, S.I., Kim, J.-Y., Nagy, H. and Zoofan, B. (1999) Effect of Pitting Corrosion on Fatigue Crack Initiation and Fatigue Life. *Engineering Fracture Mechanics*, **62**, 425-444. <https://www.sciencedirect.com/science/article/abs/pii/S0013794498001015>
- [16] Li, X., Wang, G., Kou, L., *et al.* (2024) Corrosion Pit-Induced Stress Concentration in 7005 Aluminium Alloy: Mechanical Degradation and Pit Parameter Analysis. *Engineering Fracture Mechanics*, **301**, Article 110029. <https://www.sciencedirect.com/science/article/abs/pii/S0013794424001875>
- [17] Sankaran, K.K., Perez, R. and Jata, K.V. (2001) Effects of Pitting Corrosion on the Fatigue Behavior of Aluminum Alloy 7075-T6: Modeling and Experimental Studies. *Materials Science and Engineering: A*, **297**, 223-229. <https://www.sciencedirect.com/science/article/abs/pii/S0921509300012168>
- [18] Xu, L., Yu, X., Hui, L. and Zhou, S. (2017) Fatigue Life Prediction of Aviation Aluminium Alloy Based on Quantitative Pre-Corrosion Damage Analysis. *Transactions of Nonferrous Metals Society of China*, **27**, 1353-1362.
- [19] Pidaparti, R.M., Jayanti, S., Sowers, C.A. and Palakal, M.J. (2002) Classification, Distribution, and Fatigue Life of Pitting Corrosion for Aircraft Materials. *Journal of Aircraft*, **39**, 486-492. <https://arc.aiaa.org/doi/10.2514/2.2954>